Oxidative metabolic pathway of diquat mediated by aldehyde oxidase and its detoxification effect in vitro

Zhengsheng Mao (maozhengsheng@njmu.edu.cn)
Nanjing Medical University
Youjia Yu
Nanjing Medical University
Yuxuan Wu
the First Affiliated Hospital of Nanjing Medical University
Shuainan Huang
Nanjing Medical University
Chunyan Chu
Nanjing Medical University
Qiaoyan Jiang
Nanjing Medical University
Yue Cao
Nanjing Medical University
Weiran Xie
Nanjing Medical University
Jinsong Zhang
the First Affiliated Hospital of Nanjing Medical University
Hao Sun
the First Affiliated Hospital of Nanjing Medical University
Feng Chen
Nanjing Medical University

Research Article

Keywords: Aldehyde oxidase, Diquat, Diquat monopyridone, Detoxification, Metabolism

Posted Date: May 31st, 2022

DOI: https://doi.org/10.21203/rs.3.rs-1668618/v1

Abstract

Diquat (DQ) is a fast-acting herbicide that kills both weeds and grasses and is widely used in the agricultural industry. The reported DQ poisoning cases have significantly increased in recent years. However, there is no effective antidote for the treatment of DQ poisoning. In this study, aldehyde oxidase (AOX) has been validated as the vital enzyme involved in the DQ oxidative metabolism. The metabolism of DQ to diquat monopyridone (DQ M) was significantly inhibited by AOX inhibiters including raloxifene and hydralazine. The source of oxygen atom incorporated into DQ M was proved to be from water with $H2^{18}O$ incubation experiment which further corroborated DQ M formation via AOX metabolism. The tissue distribution of DQ M *in vivo* and generation of DQ M *in vitro* by tissue co-incubation were consistent with AOX mRNA expression in tissues. The molecular docking analysis results also showed that DQ could bind to AOX. These results collectively demonstrated that AOX played a crucial in the metabolism of DQ to DQ M. Furthermore, the cytotoxicity of DQ was higher than DQ M at the same concentrations in HCCLM3, Huh7, A549, 16HBE, HEK293T and GMC cells. This study is the first to reveal the oxidative metabolic enzyme of DQ and the toxicity of DQ and its metabolite providing an important reference for clinical management of DQ poisoning.

Introduction

Diquat (DQ) is a non-selective contact herbicidal active ingredient, commonly used as a general herbicide to control weeds. Because DQ is substituted for paraquat (PQ), the cases of DQ poisoning have been gradually increasing with PQ off the market (Huang et al. 2021; Yu et al. 2022). Patients with acute DQ poisoning develop multiple organ dysfunction, especially kidney injury with tubular necrosis.

Brain injury with central pontine myelinolysis of DQ poisoning has been reported recently in a lethal DQ poisoning case (Xing et al. 2020). However, the vital enzyme involved in DQ metabolism is still unclear.

DQ monopyridone (DQ M) has been found as one of the DQ main metabolite in poisoned rats and patients (Fuke et al. 1996). The cytochrome P450 (CYP) enzymes are membrane-bound proteins that play a pivotal role in the detoxification of xenobiotics (Manikandan and Nagini 2018), which has been commonly taken as the main metabolic enzyme of DQ (Fussell et al. 2011). However, in our previous experiment, we found that DQ M was formed with rat cytosol incubation in the absence of NADPH, which was consistent with a previous study reported by Nakajima et al. (Nakajima et al. 2000).

Aldehyde oxidase (AOX) is a main cytosolic enzyme that belongs to the family of structurally related molybdo-flavoenzymes (Dalvie and Di 2019). More and more xenobiotics have been reported to be primarily metabolized by AOX (Cheshmazar et al. 2019; Uno et al. 2022), which lead to an increased recognition of the importance of AOX. In general, AOX hydroxylates the rings of various aza-, oxo-, and sulfo-hete-rocycles. There is also evidence that AOX acts not only as oxidase but also as reductase, reducing N-oxide, sufoxide, nitro-compound and heterocycle (Terao et al. 2016). As DQ contains pyridine

heterocycle and can be metabolized to DQ M in cytosolic fractions incubation without NADPH, it is reasonable to presume that AOX may be involved in the metabolism of DQ to DQ M.

In this study, we aimed to verify the role of AOX in the metabolism of DQ to DQ M. Firstly, the highly selective AOX inhibitors raloxifene (Mota et al. 2021) and hydralazine (Yang et al. 2019) were co-incubated with DQ to identify whether AOX was involved in the conversion of DQ to DQ M. Secondly, the source of oxygen atom incorporated into DQ M was studied by incubating DQ in cytosol with $H_2{}^{18}O$. Because the oxygen atoms of metabolites generated by AOX metabolism are derived from water, which is different from that of CYP metabolism from oxygen (Garattini et al. 2003). Thirdly, the tissue distribution of DQ M in rats after 1 hour of intragastric administration of DQ and the generation of DQ M after fresh tissues culturing with DQ *in vitro* were compared to AOX mRNA expression in tissues (data from GTEx database). Fourthly, the molecular docking analysis of AOX with DQ was performed with the receptor and ligand interaction function via Biovia Discovery Studio 2019 software. In addition, the cytotoxicity of DQ and DQ M were assessed by cell viability assay in HCCLM3, Huh7, A549, 16HBE, HEK293T and GMC cells. To the best of our knowledge, this is the first trial to study the metabolic enzyme of DQ and the cytotoxicity of DQ and DQ M.

Materials And Methods

Chemicals and reagents

DQ and DQ-M were obtained from J&K Scientific Ltd. (Shanghai, China). Raloxifene, hydralazine and $H_2{}^{18}O$ were purchased from Aladdin reagent Co., Ltd. (Shanghai, China). The chemical structures of DQ, DQ-M, raloxifene and hydralazine are shown in Fig. 1. The purities of all standards were above 97.0% (HPLC). Male Sprague-Dawley rats were obtained from Oriental BioService Inc. (Nanjing, China). Acetonitrile, methanol, formic acid and ammonium acetate of LC–MS grade were purchased from Sigma-Aldrich (St. Louis, MO, USA). Ultrapure water was prepared in our laboratory by ELGA LabWater system (ELGA Veolia, Bucks High Wycombe, UK). All other reagents and solvents were commercial products of analytical grade.

Preparation of rat liver cytosol

The method for preparation of rat liver cytosol has been reported in our previous study (Mao et al. 2018). Briefly, rats were sacrificed under ether anesthesia after starvation for 12h. The livers were perfused *in vivo* with ice-cold phosphate buffer via portal vein, and then quickly removed, rinsed and weighted. The liver tissues were pooled and minced, and then homogenized to 33% (w/v) in the ice-cold buffer (100 mM sodium phosphate, pH 7.4, 1.15% KCl, 250 mM sucrose and 1 mM EDTA). The homogenate was then centrifuged at 12,000 g for 20 min at 4°C. The supernatant was collected and centrifuged at 100,000 g for 60 min at 4°C using an Optima XPN-100 Ultracentrifuge (Beckman Coulter, U.S.). The resulting supernatant was collected as cytosol and then stored at -70°C. Protein concentrations were determined using commercial available Bradford protein assay kit.

Chemical inhibition experiments

To identify AOX catalyzing the conversion of DQ to DQ M, the AOX highly selective inhibitors were co-incubated with 1.0 μg/ml DQ (dissolved in normal saline) in rat liver cytosol (0.25 mg/ml), separately. The inhibitor concentrations were 1.0 μg/ml for raloxifene and 1.0 μg/ml for hydralazine. The chemical inhibitors raloxifene and hydralazine were the highly selective inhibitors of cytosolic AOX. Firstly, the rat liver cytosol was pre-incubated with raloxifene and hydralazine, respectively. After pre-incubation for 5 min, DQ was added to initiate the reaction, followed by incubation at 37°C for 30 min. The incubation was ended by adding ice-cold acetonitrile. Then, the incubation samples were centrifuged at 12,000 rpm for 5 min. Finally, 10 μL of clear upper layer was injected into the UPLC–MS/MS system for simultaneously determination of DQ and DQ M.

DQ oxidative metabolite oxygen source experiment

To confirm whether the oxygen atom incorporated into DQ M was derived from water or atmospheric oxygen, DQ (1.0 μg/mL) was incubated at 37°C in a shaking gas bath with rat liver cytosol (0.25 mg/ml) with $H_2{}^{18}O$ or H_2O, respectively. Reaction was terminated after 30 min by addition of cold acetonitrile. After mixing and centrifugation, the supernatants were analyzed by a TQ-S Micro (Waters Corp., Milford, MA, USA) triple quadrupole mass spectrometer equipped with an electrospray ionization (ESI) interface in positive ionization mode. The samples incubated with H_2O or $H_2{}^{18}O$ were analyzed using full scan mode, respectively.

Quantification of DQ M in rat tissues

All protocols were approved by the Animal Care and Ethical Committee of Nanjing Medical University. Three Sprague–Dawley (SD) rats (male, 200 ± 15 *g*, 6–8 weeks) were housed in a fixed cycle of 12 h light-dark facility with access to standard food and water. Each rat received an intragastric administration of DQ (dissolved in normal saline) at the dose of 11 mg/kg. The rats were sacrificed under ether anesthesia at 1 h after dosing, and heart, liver, lung, kidney, spleen, brain and muscle tissues were collected. All tissues (about 0.2 g per tissue) were cut into pieces and ground at 4°C with 1 mL acetonitrile. Then, the ground tissue samples were centrifuged at 12,000 rpm for 5 min. Finally, 10 μL of clear upper layer was injected into the UPLC–MS/MS system for simultaneously determination of DQ M.

Determination of metabolism of DQ in rat tissues in vitro

The rats were sacrificed under ether anesthesia, and heart, liver, lung, kidney, spleen, brain and muscle tissues were immediately collected. All tissues (about 0.1g per tissue) were cut into tiny blocks and put into six-well plate, and then added with 2 mL Dulbecco's Modified Eagle's medium (containing 1 μg/mL of DQ). The fresh tissues were cultured with DQ at 37°C for 12 h in a cell culture incubator containing 5%CO_2. Then, the culture medium samples were collected and centrifuged at 12,000 rpm for 5 min. Finally, 10 μL of clear upper layer was injected into the UPLC–MS/MS system for simultaneous determination of DQ M.

UPLC–MS/MS analysis

The method for determination of DQ and DQ M has been developed and validated by our previous study (Mao et al. 2022). Briefly, the UPLC–MS/MS analyses were performed with a TQ-S Micro (Waters Corp., Milford, MA, USA) triple quadrupole mass spectrometer in the electrospray ionization (ESI) mode. The chromatographic separation was carried out using a CORTECS® UPLC® HILIC (100 mm × 2.1 mm, 1.6 μm) column (Waters Corp., Milford, MA, USA) at 40°C. The mobile phase composed of a mixture of 10 mM ammonium acetate with 0.5% formic acid (water phase) and acetonitrile (organic phase) was used at a flow rate of 0.35 mL/min. The step-wise elution was as follows: 70% organic phase (0-0.50 min), 30% organic phase (0.51–1.60 min), 70% organic phase (1.61–2.50 min). The source gas (nitrogen) flow was 660 L/hr, cone flow was 33 L/hr, desolvation temperature at 460°C, cone voltage was 35 V, and capillary voltage was 1.0 kV. The quantification m/z transitions of 183.1→156.6 and 199.1→155.1 and qualification m/z transitions of 183.1→129.5 and 199.1→78.3 were chosen for monitoring DQ and DQ-M, respectively

Molecular docking

The crystal structure of AOX (PDB: 4UHW) was downloaded from the Protein Data Bank website (https://www.rcsb.org). All crystallographic water and ligands were removed from the protein using the Biovia Discovery Studio 2019 software. Then, the receptor model was optimized by protein automatic preparation function. The 3D structure of DQ was prepared via PerkinElmer Chem3D 18.0 software. The optimized structure of DQ with energy minimization was defined as docking ligand. Finally, the docking analysis of AOX with DQ was performed with the receptor and ligand interaction function via Biovia Discovery Studio 2019 software

Cell viability assay

Cell viability was assessed using the WST-1 Cell Proliferation Assay Kit (Beyotime, Shanghai, China). HCCLM3, Huh7, A549, 16HBE, HEK293T and GMC cells (100 μL) were cultured in 96-well plates (1×10^3 cells/well) for 24 h and then treated with different concentrations at 0, 50, 100 and 200 μg/mL of DQ or 0, 50, 100 and 200 μg/mL of DQ M for 24 h. Following treatment, 10 μL of the reconstituted WST-1 mixture was added to each well, mixed gently for one minute on an orbital shaker, and incubated for 2 h at 37°C in a CO_2 incubator. Absorbance was measured at 450 nm using a microplate reader.

Results And Discussion

Chemical inhibition experiments

Although the previous studies mentioned that CYP450 enzymes might be responsible for the metabolism of DQ (Fussell et al. 2011), there was no experimental evidence yet. In our previous experiment, we found that DQ M was formed with rat cytosol in the absence of NADPH, indicating that the reaction was localized in cytosolic fractions and NADPH-independent. Thus, it is reasonable to presume that non-

CYP450 enzymes such as AOX might be involved in the metabolism of DQ to DQ M. To identify AOX catalyzing the conversion of DQ to DQ M, the AOX highly selective inhibitors raloxifene and hydralazine were co-incubated with 1.0 μg/ml DQ (dissolved in normal saline) in rat liver cytosol (0.25 mg/ml), seperately. After incubation of DQ and cytosol with or without AOX inhibitors at 37°C for 30 min, the residual amount of DQ had a significant increase in both AOX inhibitor groups (Fig. 2a), while the amount of DQ M dropped dramatically in AOX inhibitor groups (Fig. 2b).

The source of oxygen atom incorporated into DQ M

DQ was incubated with rat liver cytosol in the presence of $H_2{}^{18}O$ or H_2O. LC-MS/MS analysis indicated that the oxygen incorporated into DQ M was derived from $H_2{}^{18}O$. The molecular ion of DQ M ($[M]^+$) appeared at m/z 199 in H_2O incubation (Fig. 3c), while the corresponding ions showed 2-atomic mass units higher at m/z 201 in $H_2{}^{18}O$ incubation (Fig. 3c), indicating that water is the source of the oxygen atom incorporated into DQ M. This is consistent with the oxidative mechanism of AOX (Fig. 3a) (Garattini et al. 2003). The source of oxygen atom incorporated into DQ M was proven from water which further corroborated DQ M formation via AOX metabolism.

Distribution of DQ M in rat tissues

The rats were sacrificed under ether anesthesia, and the heart, liver, lung, kidney, spleen, brain and muscle were collected after 1 h of intragastric administration of DQ (11 mg/kg). The established UPLC-MS/MS method was used to analyze tissue samples containing DQ M in parallel with blank tissue controls, and the obtained data were processed using MassLynx V4.1 software. The quantification m/z transitions of 199.1→155.1 and qualification m/z transitions of 199.1→78.3 were chosen for monitoring DQ-M, respectively. As shown in Fig. 4a, DQ M was widely distributed in heart, liver, lung, kidney, spleen, brain and muscle.

Metabolism of DQ in rat tissues in vitro

The fresh blocks of heart, liver, lung, kidney, spleen, brain and muscle tissues of rats were cultured with DQ (1 μg/mL) at 37°C for 12 h in a cell culture incubator, respectively. Then, the culture medium samples were collected and analyzed by the established UPLC-MS/MS method, and the obtained data were processed using MassLynx V4.1 software. The quantification m/z transitions of 199.1→155.1 and qualification m/z transitions of 199.1→78.3 were chosen for monitoring DQ-M, respectively. As shown in Fig. 4b, DQ M was generated in heart, liver, lung, kidney, spleen, brain and muscle tissues cultured with DQ. The results of tissue distribution of DQ M *in vivo* and generation of DQ M by tissue co-incubation *in vitro* were consistent with the AOX mRNA expression in tissues (Fig. 4c, data from GTEx database). These result further validated DQ M formation via AOX metabolism.

Molecular docking

Molecular docking study was carried out on the DQ with AOX protein target 4UHW. The docking results showed that DQ molecule bound to AOX protein with residues ARG58, SER80, ILE265, SER287, MET266,

PRO288, LEU294, ILE291, ARG290, GLY309, SER295 and ASP289. ARG58, SER80, ILE265, SER287, PRO288, ILE291, GLY309 and SER295 have been showed to have van der waals interaction with DQ. ASP289 had attractive charge and ARG290 had unfavorable positive-positive interaction with DQ. In addition, ARG290 also had pi-sigma, MET266 had pi-sulfur and LEU294 had pi-alkyl interaction with DQ. The 3D and 2D interaction between DQ and AOX were visualized using Biovia Discovery Studio 2019 (Fig. 5).

Cytotoxicity of DQ and DQ M on six types of cells

To compare the cytotoxicity of DQ with DQ M, HCCLM3, Huh7, A549, 16HBE, HEK293T and GMC cells were exposed to DQ and DQ M at the same concentrations for 24 h. Cell viability was assessed using the WST-1 Cell Proliferation Assay Kit. The WST-1 results showed that cell viabilities of six types of cells were all higher in DQ M groups than that in DQ groups with the same concentration treatments (Fig. 6). Thus, the oxidative metabolism of DQ to DQ M by AOX is a detoxification metabolic process.

Conclusions

In this study, AOX has been proved to be the key enzyme in the metabolism of DQ to DQ M. The AOX selective inhibitors, the source of oxygen atom incorporated into DQ M, the tissue distribution of DQ M *in vivo* and the generation of DQ M after fresh tissues culturing with DQ and the molecular docking analysis of AOX with DQ were carried out, which jointly confirmed that aldehyde oxidase mediates the oxidative metabolism of DQ to DQ M. In addition, the cytotoxicity studies results showed that cell viabilities of six types of cells were all higher in DQ M groups than DQ groups with the same concentration treatments, which meant that the oxidative metabolism of DQ to DQ M by AOX is a detoxification metabolic process *in vitro*. To the best of our knowledge, this work is the first to ascertain the metabolic enzyme of DQ, and provides information that AOX would be an important target for the treatment of DQ poisoning.

Declarations

Author contribution The experiments of this work were designed by Zhengsheng Mao, Youjia Yu and Yuxuan Wu. The experiments were performed by Shuainan Huang, Chunyan Chu, Qiaoyan Jiang and Yue Cao. Weiran Xie, Jinsong Zhang, Hao Sun and Feng Chen analyzed the data and edited the figures. The first draft of the manuscript was written by Zhengsheng Mao and all authors commented on previous versions of the manuscript. All authors read and approved the final manuscript.

Funding This work was supported by the Natural Science Research of Jiangsu Higher Education Institutions of China (Grant No. 20KJB340001), the Natural Science Foundation of Jiangsu Province (Grant No. BK20201351), the National Natural Science Foundation of China (Grant No. 82002028, 81772020, 82072158 and 21904068).

Conflict of interest The authors declare that there are no conflicts of interest.

Ethics approval The SD rats used in this study were maintained according to European guidelines on the protection of animals used for scientific purposes (Directive 2010/63/EU). All animal handling procedures used in this study were approved by the Animal Care and Ethical Committee of Nanjing Medical University.

References

1. Cheshmazar N, Dastmalchi S, Terao M, Garattini E, Hamzeh-Mivehroud M (2019) Aldehyde oxidase at the crossroad of metabolism and preclinical screening. Drug metabolism reviews, 51(4), 428–452. https://doi.org/10.1080/03602532.2019.1667379
2. Dalvie D, Di L (2019) Aldehyde oxidase and its role as a drug metabolizing enzyme. Pharmacology & therapeutics, 201, 137–180. https://doi.org/10.1016/j.pharmthera.2019.05.011
3. Fuke C, Ameno K, Ameno S, Kinoshita H, Ijiri I (1996) Detection of two metabolites of diquat in urine and serum of poisoned patients after ingestion of a combined herbicide of paraquat and diquat. Arch Toxicol 70(8):504–507. doi: 10.1007/s002040050305
4. Fussell KC, Udasin RG, Gray JP, Mishin V, Smith PJ, Heck DE et al (2011) Redox cycling and increased oxygen utilization contribute to diquat-induced oxidative stress and cytotoxicity in Chinese hamster ovary cells overexpressing NADPH-cytochrome P450 reductase. Free radical biology & medicine, 50(7), 874–882. https://doi.org/10.1016/j.freeradbiomed.2010.12.035
5. Garattini E, Mendel R, Romão MJ, Wright R, Terao M (2003) Mammalian molybdo-flavoenzymes, an expanding family of proteins: structure, genetics, regulation, function and pathophysiology. The Biochemical journal, 372(Pt 1), 15–32. https://doi.org/10.1042/BJ20030121
6. Huang Y, Zhang R, Meng M, Chen D, Deng Y (2021) High-dose diquat poisoning: a case report. The Journal of international medical research, 49(6), 3000605211026117. https://doi.org/10.1177/03000605211026117
7. Mao Z, Yu Y, Sun H et al (2022) Simultaneous determination of diquat and its two primary metabolites in rat plasma by ultraperformance liquid chromatography-tandem mass spectrometry and its application to the toxicokinetic study. Forensic Toxicology. https://doi.org/10.1007/s11419-022-00623-z
8. Mao Z, Wu Y, Li Q, Wang X, Liu Y, Di X (2018) Aldehyde oxidase-dependent species difference in hepatic metabolism of fasudil to hydroxyfasudil. Xenobiotica; the fate of foreign compounds in biological systems, 48(2), 170–177. https://doi.org/10.1080/00498254.2017.1292016
9. Manikandan P, Nagini S (2018) Cytochrome P450 Structure, Function and Clinical Significance: A Review. Current drug targets, 19(1), 38–54. https://doi.org/10.2174/1389450118666170125144557
10. Mota C, Diniz A, Coelho C, Santos-Silva T, Esmaeeli M, Leimkühler S et al (2021) Interrogating the Inhibition Mechanisms of Human Aldehyde Oxidase by X-ray Crystallography and NMR Spectroscopy: The Raloxifene Case. Journal of medicinal chemistry, 64(17), 13025–13037. https://doi.org/10.1021/acs.jmedchem.1c01125

11. Nakajima M, Nagao M, Iwasa M, Monma-Ohtaki J, Maeno Y, Koyama H, et al (2000) Purification and characterization of diquat (1,1'-ethylene-2, 2'-dipyridylium)-metabolizing enzyme from paraquat-resistant rat liver cytosol. Toxicology, 154(1–3), 55–66. https://doi.org/10.1016/s0300-483x(00)00299-7
12. Terao M, Romão MJ, Leimkühler S, Bolis M, Fratelli M, Coelho C et al (2016) Structure and function of mammalian aldehyde oxidases. Archives of toxicology, 90(4), 753–780. https://doi.org/10.1007/s00204-016-1683-1
13. Uno Y, Uehara S, Yamazaki H (2022) Drug-oxidizing and conjugating non-cytochrome P450 (non-P450) enzymes in cynomolgus monkeys and common marmosets as preclinical models for humans. Biochemical pharmacology, 197, 114887. https://doi.org/10.1016/j.bcp.2021.114887
14. Xing J, Chu Z, Han D, Jiang X, Zang X, Liu Y, et al (2020) Lethal diquat poisoning manifesting as central pontine myelinolysis and acute kidney injury: A case report and literature review. J Int Med Res 48(7):1–6. doi: 10.1177/0300060520943824
15. Yang X, Johnson N, Di L (2019) Evaluation of Cytochrome P450 Selectivity for Hydralazine as an Aldehyde Oxidase Inhibitor for Reaction Phenotyping. Journal of pharmaceutical sciences, 108(4), 1627–1630. https://doi.org/10.1016/j.xphs.2018.11.007
16. Yu G, Jian T, Cui S, Shi L, Kan B, Jian X (2022) Acute diquat poisoning resulting in toxic encephalopathy: a report of three cases. Clinical toxicology (Philadelphia, Pa.), 60(5), 647–650. https://doi.org/10.1080/15563650.2021.2013495

Figures

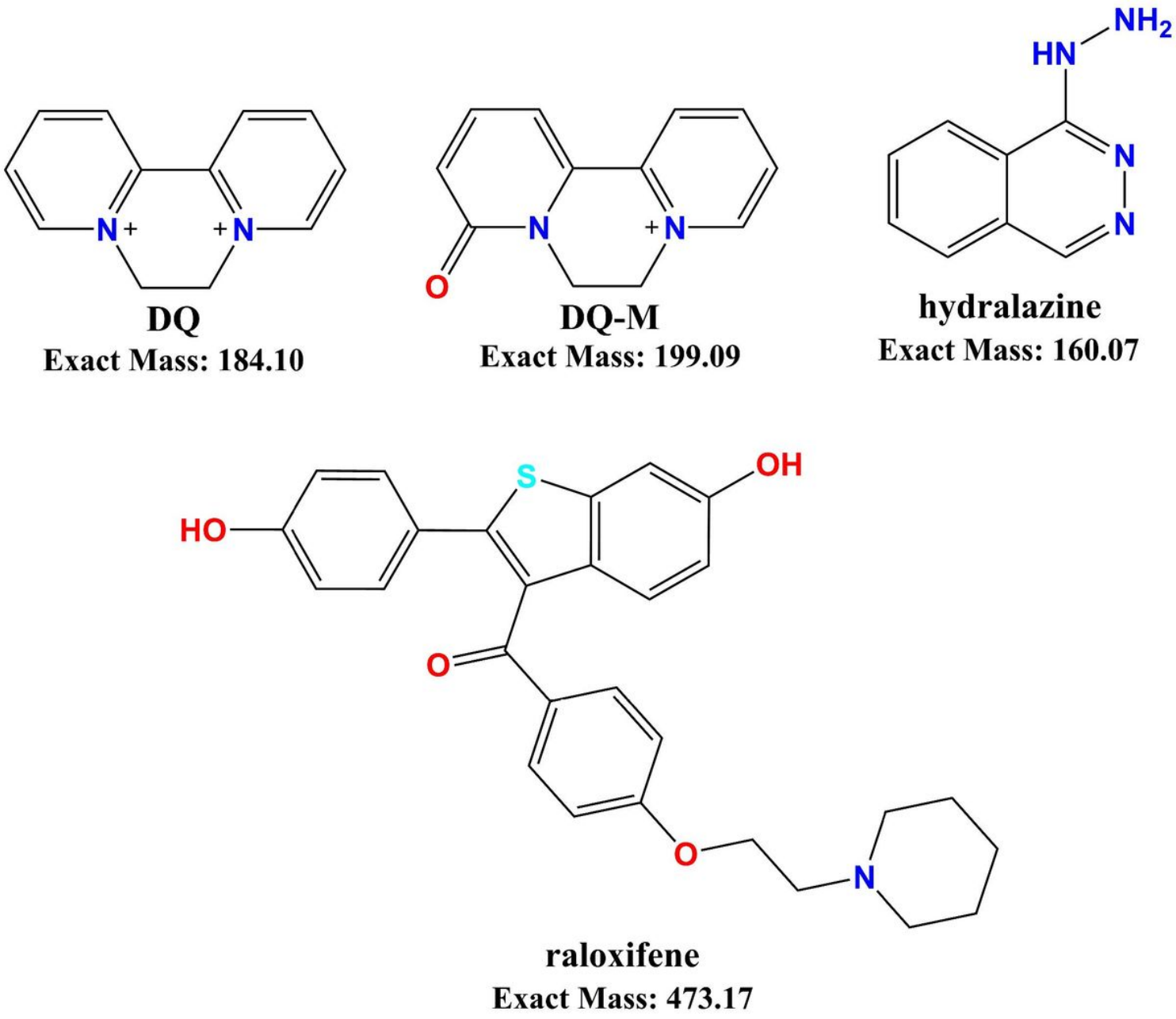

Figure 1

Structures of DQ, DQ M, hydralazine and raloxifene

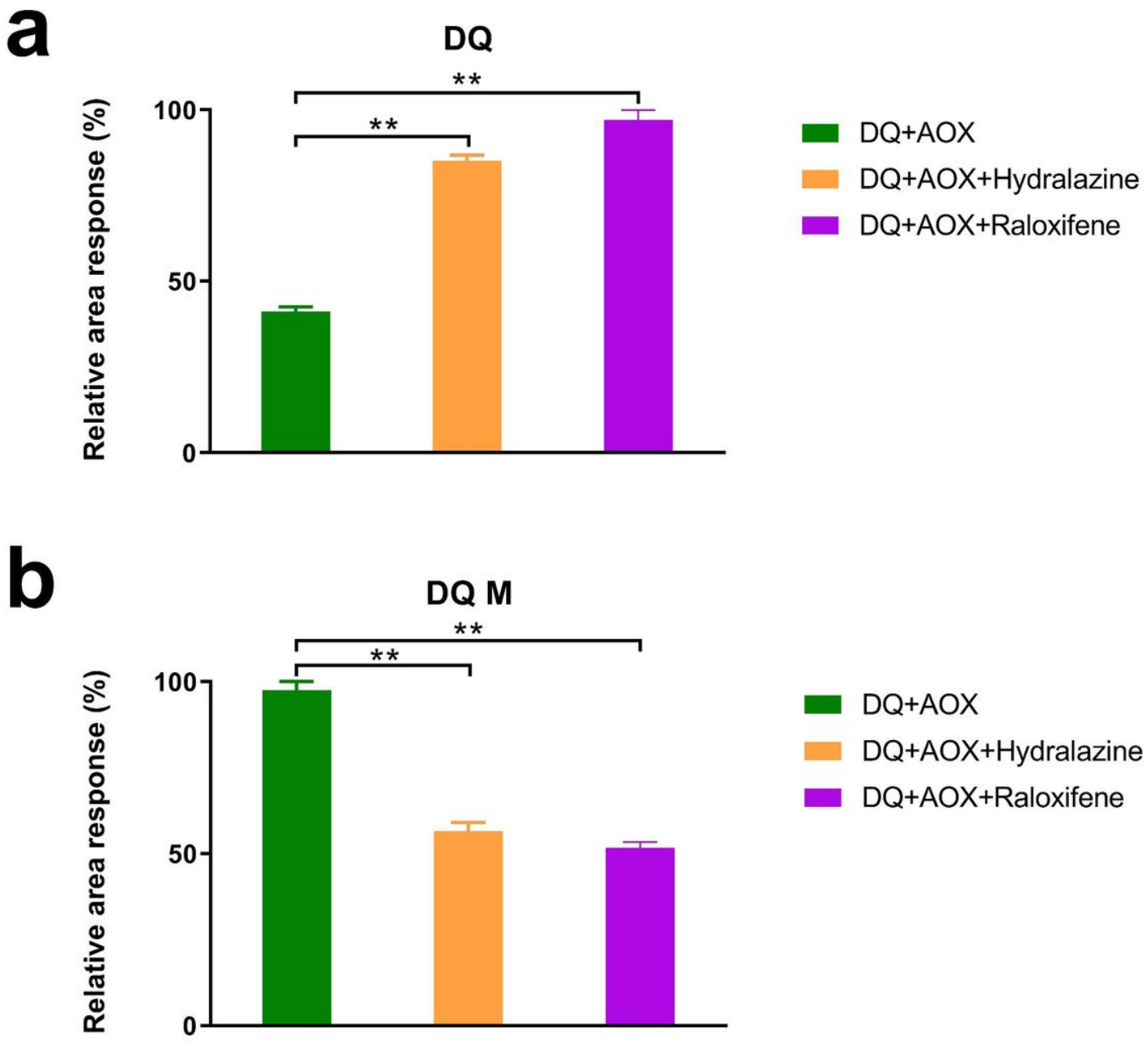

Figure 2

The relative area response of **a** DQ, **b** DQ M after DQ incubation with AOX and AOX inhibitors. Signifcant diferences compared with the control were marked with asterisks, **P<0.001

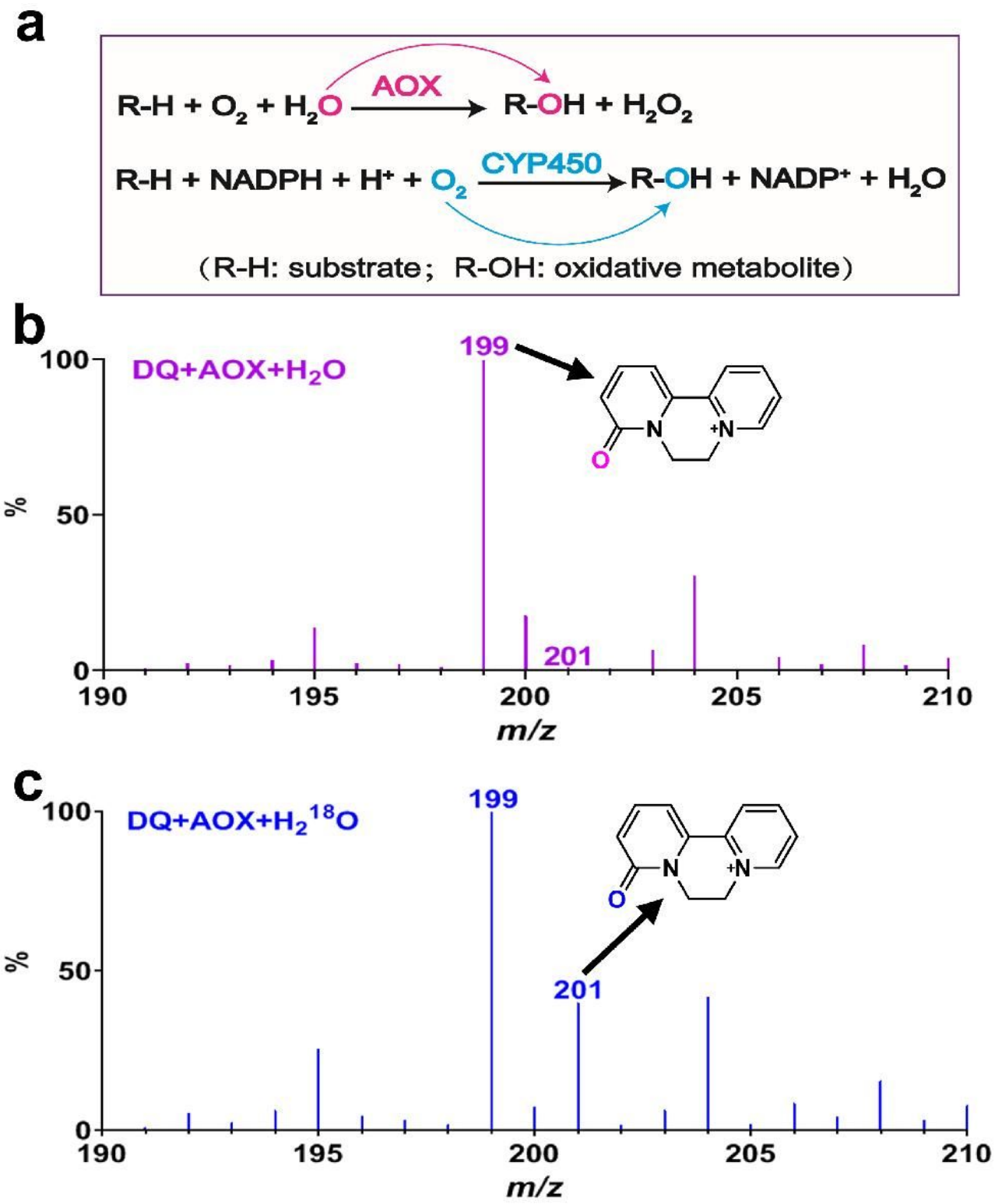

Figure 3

a the oxidative mechanism of AOX and CYP150, **b** the full mass scan of DQ M after DQ culturing with rat liver cytosol in the presence of H_2O, **c** the full mass scan of DQ M after DQ culturing with rat liver cytosol in the presence of $H_2{}^{18}O$

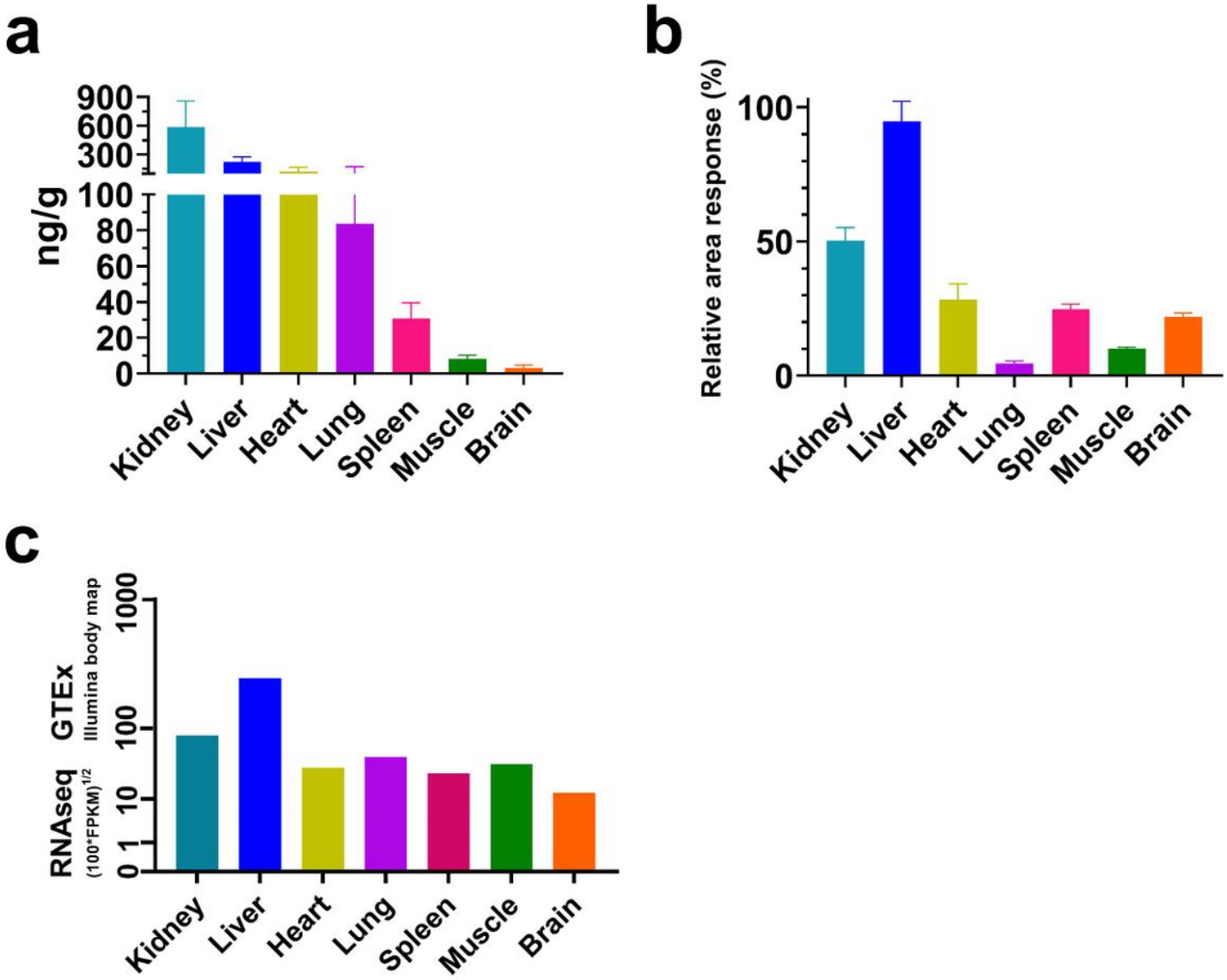

Figure 4

a the tissue distribution of DQ M in rats after 1 hour of intragastric administration of DQ, **b** the generation of DQ M after fresh tissues culturing with DQ *in vitro*, **c** the AOX mRNA expression in tissues (data from GTEx database)

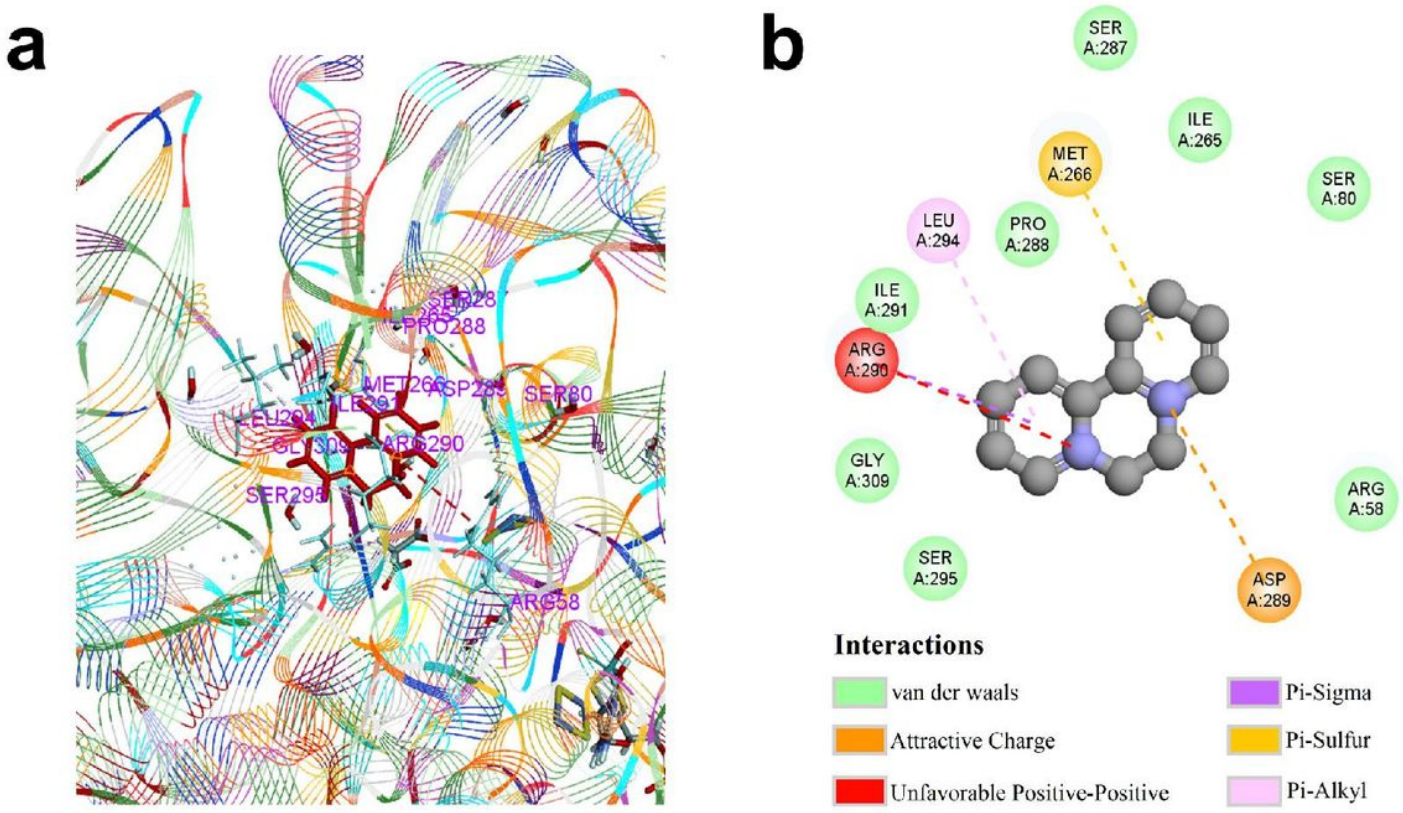

Figure 5

a The 3D interaction between DQ and corresponding active sites of AOX, **b** The 2D interaction between DQ and corresponding active sites of AOX

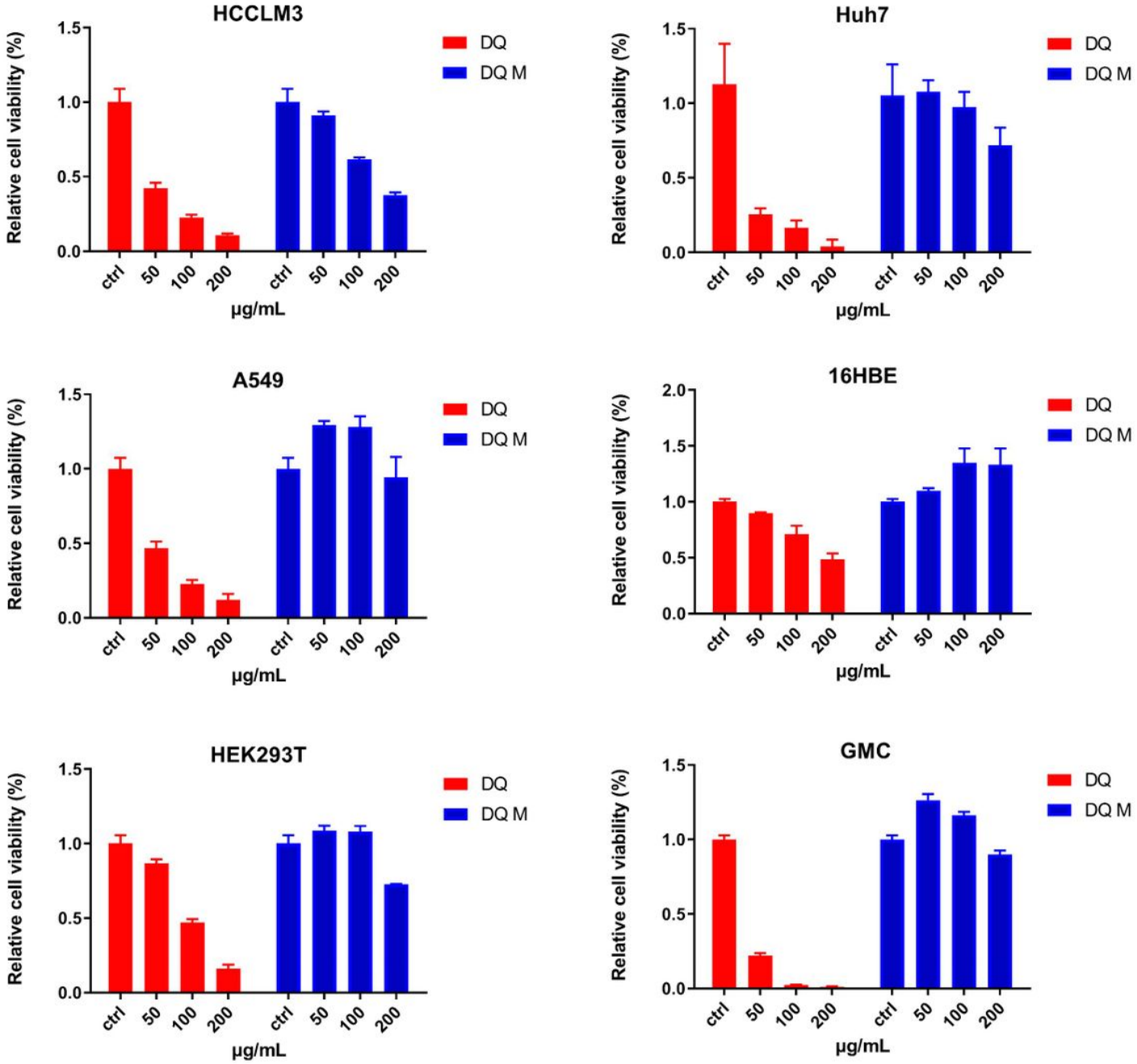

Figure 6

the cytotoxicity of DQ and DQ M in six types of cells